

Analysis of Gene Expression Patterns in Systemic Sclerosis Fibroblasts Using RNA Arbitrarily Primed-Polymerase Chain Reaction for Differential Display

ROTRAUD MEYRINGER, ELENA NEUMANN, MARTIN JUDEX, MICHAEL LANDTHALER, FRANK KULLMANN, JÜRGEN SCHÖLMERICH, STEFFEN GAY, INGO H. TARNER, OLIVER DISTLER, and ULF MÜLLER-LADNER

ABSTRACT. *Objective.* To identify genes that are differentially expressed in systemic sclerosis (SSc) fibroblasts of clinically involved and noninvolved skin compared to normal dermal fibroblasts, using RNA arbitrarily primed-polymerase chain reaction (RAP-PCR) for differential display.

Methods. We examined 12 fibroblast cultures derived from clinically involved skin, 3 fibroblast cultures from noninvolved skin, and 4 fibroblast cultures from healthy skin. After extraction of total RNA, the first step of RAP-PCR was performed using different arbitrary 10–12-base primers for first-strand cDNA synthesis. Second-strand synthesis was achieved by cycling using different arbitrary 10-base primers, followed by sequence analysis of the amplified fingerprint products. The resulting sequences were aligned to the GenBank® database using Blast® Search. Confirmation of differential expression was performed with specific primers using real-time PCR.

Results. Using 8 different primer combinations, in total 48 cDNA were differentially expressed between SSc and healthy dermal fibroblasts. Sequence analysis identified distinct PCR products, which were overexpressed in SSc as highly homologous to gene segments of gremlin protein, lysyl oxidase, c-cbl proto-oncogene, an estrogen-responsive element, fibronectin, and collagen type XII α 1 precursor.

Conclusion. Our results show that RAP-PCR is a suitable method to identify differentially expressed genes in SSc fibroblasts. Further, we identified genes that have not yet been described in the pathophysiology of SSc and that may be involved in matrix synthesis and cellular interaction. (J Rheumatol 2007;34:747–53)

Key Indexing Terms:

SYSTEMIC SCLEROSIS FIBROBLASTS GENE EXPRESSION DIFFERENTIAL DISPLAY

Increased production of extracellular matrix proteins by fibroblasts, especially collagen, is a typical histopathologic feature in systemic sclerosis (SSc), followed by an irreversible thickening of connective tissue and loss of function of internal organs. Little is known about specific regulation of genes

and pathways leading to this increased matrix synthesis. However, recent data suggest an activation of distinct pathways in diseased skin of patients with SSc.

Our aim was to identify genes that are specifically expressed or upregulated in SSc dermal fibroblasts, and that may be linked to the pathophysiology of the disease. Recently, various strategies have been developed to examine differences in tissue-specific gene expression. Among them, differential display for RNA arbitrarily primed-polymerase chain reaction (RAP-PCR) has been proven to be both efficient and reliable for numerous experimental settings including malignant¹ and nonmalignant inflammatory diseases². We analyzed the potential of RAP-PCR for evaluation of differential expression of RNA of SSc fibroblasts of clinically involved and noninvolved skin as compared to normal dermal fibroblasts.

MATERIALS AND METHODS

Patients and skin biopsies. Skin biopsies were obtained from involved skin of 12 patients with SSc, 6 with limited disease (lSSc) and 6 with diffuse disease (dSSc), and from noninvolved skin of 3 patients. All patients met the preliminary criteria for SSc of the American College of Rheumatology³. All patients gave informed consent for the biopsies, and the study was approved by the local ethics committee. SSc samples were compared to skin biopsies taken from healthy skin of 4 individuals during routine surgery.

Cell culture. Dermal fibroblasts were enzymatically extracted from the biopsies and cultured under the same conditions. After enzymatic digestion and

From the Department of Internal Medicine I and Department of Dermatology, University of Regensburg; Department of Rheumatology, Asklepios Clinic Bad Abbach; Department of Rheumatology and Clinical Immunology, Kerckhoff Clinic Bad Nauheim/University of Giessen; Max-Planck Institute for Biochemistry, München, Germany; and Center for Experimental Rheumatology, University of Zürich, Zürich, Switzerland.

Supported by grants of the German Scleroderma Foundation and the German Research Society (DFG, Mu 1383/1-3 and Ku 1024/6-3).

R. Meyringer, MD, Department of Internal Medicine I, University of Regensburg and Department of Rheumatology, Asklepios Clinic Bad Abbach; E. Neumann, PhD; I.H. Turner, MD; U. Müller-Ladner, MD, Department of Rheumatology and Clinical Immunology, Kerckhoff Clinic Bad Nauheim/University of Giessen; M. Judex, PhD, Department of Internal Medicine I, University of Regensburg and Max-Planck Institute for Biochemistry; M. Landthaler, MD, Department of Dermatology, University of Regensburg; F. Kullmann, MD; J. Schölmerich, MD, Department of Internal Medicine I, University of Regensburg; S. Gay, MD; O. Distler, MD, Center for Experimental Rheumatology, University of Zurich.

Address reprint requests to Dr. U. Müller-Ladner, Department of Rheumatology and Clinical Immunology, University of Giessen and Kerckhoff Clinic Bad Nauheim, Benekestrasse 2-8, D-61231 Bad Nauheim, Germany. E-mail: u.mueller-ladner@kerckhoff-klinik.de

Accepted for publication December 13, 2006.

removal of nonadherent cells, fibroblasts were grown in Dulbecco's modified Eagle's medium (Biochrom, Berlin, Germany) containing 10% heat inactivated fetal calf serum, 100 U/ml penicillin, and 0.1 mg/ml streptomycin (PAA Laboratories, Linz, Austria). Cells were cultured at 37°C in 10% CO₂. Cultures were routinely tested for mycoplasma contamination.

RNA extraction. At 80%–90% confluency, cultured fibroblasts were harvested after 4–8 passages and total cellular RNA was extracted by silica gel binding using the RNeasy spin column purification kit (Qiagen, Hilden, Germany). To remove remaining genomic DNA, total RNA was treated with DNase I (0.2 U/μl; Boehringer Mannheim, Germany) for 30 min at room temperature. RNA concentrations were measured using the Ribogreen RNA quantification kit (Molecular Probes, Leiden, Netherlands), and stored at –70°C. Equal aliquots were then electrophoresed on 1% agarose gels stained with ethidium bromide to compare large and small rRNA qualitatively, and to exclude degradation.

RAP-PCR of total cellular RNA. RAP-PCR of total cellular RNA was performed as described². Three different concentrations of RNA were used as template for each experiment to exclude concentration-dependent artefacts and to test the reproducibility of the RNA fingerprint. The first step of RAP-PCR was performed using MMuLV reverse transcriptase (Promega, Madison, WI, USA) and 2 μM of 2 different first-strand arbitrary 10mer primers (US6 5'-GTG GTG ACA G-3', US9 5'-GTG ACA GAC A-3') for reverse transcription. Second-strand synthesis was achieved by cycling at low stringency conditions (30 s at 94°C, 30 s at 35°C, 30 s at 72°C) for 35 cycles using AmpliTaq Stoffel Fragment (Perkin Elmer, Norwalk, CT, USA) and 4 μM of a different arbitrary primer (Nuclear 1+ 5'-ACG AAG AAG AG-3', OPN21 5'-ACC AGG GGC A-3', OPN29 5'-CAC CAG GGG C-3', KinaseA2+ 5'-GGT GCC TTT GG-3'). Eight different primer combinations were used. For separation of the PCR products, 3 μl of the PCR reaction were denatured (94°C for 3 min) and loaded onto 8 M urea/6% polyacrylamide sequencing gels. Gels were then transferred to 3MM Whatman paper, dried under vacuum at 80°C, and exposed directly to Kodak BioMax[®] autoradiography film (Kodak, Stuttgart, Germany) at room temperature for 24 h.

Cloning. Differentially expressed bands were cut out from the gel and PCR products were eluted by soaking the gel fragments in Tris buffer. After further purification through SSCP gel electrophoresis and verification of its correct size and purity on 4% agarose gels, the PCR product of interest was cloned into PCR[®]-II TOPO vector using the TOPO-TA-Cloning[®] Kit (Invitrogen, De Schelp, Netherlands). Three clones per transcript were sequenced. The resulting sequences were aligned to the GenBank[®] database using Blast[®] Search.

Real-time PCR. Real-time PCR was performed using the LightCycler system (Roche Diagnostics, Mannheim, Germany) according to the instructions of the manufacturer. Reactions were performed in a 20 μl volume containing 0.5 μM primers, 2–4 mM MgCl₂, and 2 μl LightCycler-FastStart SYBR Green I reaction mix (Roche). After 10 min polymerase activation at 95°C, 40 cycles with denaturation at 95°C for 15 s, annealing at 52°C for 5 s, and extension at 72°C for 20 s were performed. Fluorescence was measured at the end of the 72°C extension period. Specific primers were designed for the genes of interest. The sequences of the designed primers are shown in Table 1.

Efficiencies of the primers were tested using the standard curve method ($E = 10^{-1/\text{slope}}$). According to the guidelines of the manufacturer, efficiencies of 2.00 ± 0.05 were considered acceptable for experiments. Efficiencies of primer pairs for relative quantification were identical or met the above mentioned standard. To confirm amplification specificity, PCR products were subjected to a melting curve analysis. The data were analyzed using the LightCycler software as described by the manufacturer. The baseline of each reaction was equalized by calculating the mean value of the 5 lowest measured data points for each sample and subtracting these values from each reading point. Background fluorescence was removed by setting a noise band. In this approach, the cycle number at which the best-fit line through the log-linear portion of each amplification curve intersects the noise band is inversely proportional to the log of copy numbers^{4,5}. The crossing points are the intersections between the best-fit lines of the log-linear region and the noise band.

Table 1. Primer pairs used for amplification of the individual differently expressed genes identified by RAP-PCR (for: forward, rev: reverse).

Primer	Sequence
cbl for	5'-GAA TTA TAC TGT GAG ATG GGC-3'
cbl rev	5'-CAG CCA ATT CCT TCA TCA TGA-3'
Col 12 for	5'-CAC AAT ACG CCT TAT CTG TG-3'
Col 12 rev	5'-GAG ATA ATT CAG TTG TGG CA-3'
DAGK for	5'-GTT CAA CCT CCT AAA GGA TG-3'
DAGK rev	5'-CAC GCC AAT AGA GAA GTA GT-3'
Fibronectin for	5'-CCA AGA AGT GAC TCG CTT TG-3'
Fibronectin rev	5'-GCG CTG TTG TTT GTG AAG TA-3'
PLCG1 for	5'-GGA TGA GTT TGT CAC CTT CC-3'
PLCG1 rev	5'-GTC CTC AAT GGA CAG GAT GA-3'
MLN for	5'-GAT CGG AAG AAT CCA GCA TA-3'
MLN rev	5'-GTA CCT GCA GCA TTC CTG TT-3'
MEGF for	5'-CAG TAA AGG CAT AAT CAG GC-3'
MEGF rev	5'-CAT CTG ATA GCT CCT CTG TG-3'
efp for	5'-GAT GAT GTG AGA AAC AGG CAG CAG G-3'
efp rev	5'-TTC AGT TCC ACC TCG GGG ATG TAG-3'
Zinc for	5'-GCA TCT GCC ACA TCT GCC TG-3'
Zinc rev	5'-GCT GTT GAC CCT CTT CTC CTC TTC-3'
Gremlin for	5'-CAC TAC CAT GAT GGT CAC AC-3'
Gremlin rev	5'-CTC TCT AGC AGA GAC TGT GT-3'
Lysyloxidase for 2	5'-GCT GGC TAC TCG ACA TCT AG-3'
Lysyloxidase rev 2	5'-GTA TGC TGT ACT GGC CAG AC-3'

RAP-PCR: RNA arbitrarily primed - polymerase chain reaction; Cbl: c-Cbl proto-oncogene; DAGK: diacylglycerol kinase; PLCG1: phospholipase Cγ1; MEGF: murine epidermal growth factor; MLN: metastatic lymph node.

Statistical analysis. Significance of differential expression was calculated using the Wilcoxon rank-sum test. p values < 0.05 were regarded as significant.

RESULTS

RAP-PCR. On average, 70 different RNA were obtained per primer pair, of which most were expressed by all dermal fibroblasts — in SSc as well as in normal skin. Using 8 different primer combinations, in total 48 cDNA were found to be differentially expressed between SSc and normal dermal fibroblasts. Of these, strong amplification of 13 distinct PCR products suitable for sequencing could be obtained. The autoradiography of a RAP-PCR gel is shown in Figure 1; the arrow indicates one of the cDNA fragments, which was subjected to sequence analysis.

Cloning and sequencing of the differentially amplified RAP-PCR products. Sequence analysis identified the 45 PCR products as highly homologous to segments of mRNA for known proteins or to segments of DNA clones. Figure 2 illustrates the result of the comparison of the homology of 2 gene fragments, gremlin and fibronectin (precursor). A synopsis of the differentially expressed genes is shown in Table 2. The majority of the PCR products were found to be upregulated in SSc. All proteins for which a relation to extracellular matrix production is known are marked in bold. Two genes found to be downregulated in SSc fibroblasts corresponded to gene segments of

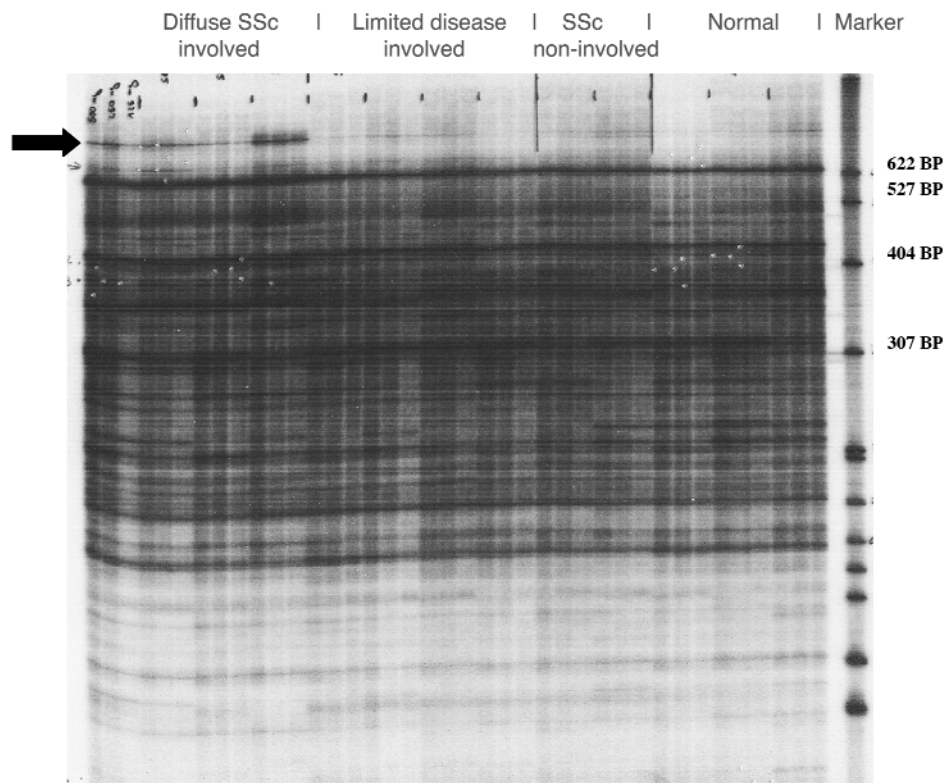


Figure 1. RNA fingerprint from skin fibroblasts from involved and noninvolved skin of patients with diffuse and limited SSc and from healthy skin, using US6 and OPN23 primer for amplification. The arrow shows one of the differentially expressed genes in patients with dSSc represented by a distinct PCR product.

ribosomal proteins. The remaining 3 sequences shared only partial or no homology to known genes.

Of the genes that are known to be involved in matrix metabolism, and that were found to be dysregulated in SSc fibroblasts, 8 were subjected to confirmation of differential expression by real-time PCR: (1) an estrogen-responsive finger protein (*efp147*); (2) *c-Cbl* proto-oncogene; (3) gremlin protein; (4) phospholipase *Cyl*; (5) diacylglycerol kinase (*DAGK*); (6) lysyl oxidase; (7) fibronectin precursor; and (8) collagen type $\text{XII}\alpha 1$. They all were found to be upregulated in SSc.

Real-time PCR. Confirmation of differential expression was performed with specific primers using real-time PCR with the LightCycler system. Of the 9 genes noted above, true differential expression could only be shown for gremlin protein and lysyl oxidase (Figure 3). Lysyl oxidase was found to be differentially upregulated between involved skin of dSSc and ISSc versus uninvolved skin ($p < 0.044$) and versus normal skin ($p < 0.004$) (Figure 3A). On the other hand, gremlin protein was also found to be differentially regulated between involved skin of patients with dSSc and ISSc versus uninvolved skin ($p < 0.048$) (Figure 3B). In contrast, differential expression could not be confirmed for the remaining genes (data not shown).

DISCUSSION

Aside from its numerous applications for examining malignant tissues and cells for different gene expression¹, although being in the era of cDNA arrays, RAP-PCR for fingerprinting has proven its reliability to identify novel genes in nonmalignant and inflammatory diseases^{2,6}. However, this is the first study to show the value of this technique in a slowly progressing autoimmune connective tissue disease.

Among the different genes that were found to be upregulated in SSc in general, precursors of extracellular matrix proteins, collagen, and fibronectin could be identified. As noted above, increased accumulation of extracellular matrix proteins in the dermis is a histopathologic feature of SSc, and the increased collagen and fibronectin production of dermal fibroblasts in SSc has been shown in various experimental approaches^{7,8}. Thus, the finding of an overexpression of these matrix proteins reflects the reliability of the method. Of the other genes found to be upregulated in SSc, a link to the disease has been described only in single cases — hitherto the majority showed no known association to SSc. Of these genes that appear to be directly involved in the synthesis of extracellular matrix, 5 were selected for further confirmation: lysyl oxidase, gremlin protein, *cCbl*, *DAGK*, and phospholipase *Cyl*.

Table 2. Synopsis of all differently expressed genes and their respective proteins.

Clone no.	Gene/Correlating Protein	Identifying Clones	Expression	GenBank no.
A1.1	Chromosome 11, clone RP 11-2C23	—	+ Normal	AC015684
A1.2	Chromosome 20, clone RP1-18C9	—	+ Normal	AL049709
A1.3	Chromosome 6, clone RP3-493H23	—	+ Normal	AL121789
A2.1	Chromosome 5, clone CTB-47B11	—	+ SSc	AC008676
A2.2	Interleukin 17 receptor	—	+ SSc	NM_014339
A2.3	Chromosome 1, clone 598F2	—	+ SSc	AL021579
A3.1, 3.3, B1.1, 1.3, C1.1	Chromosome 10, clone RP11-399019	5/9	+ SSc	AL157394
A3.2	Chromosome 22, clone RP 5-979N1	—	+ SSc	AL035659
A4, B2.3	Chromosome 9, clone RP11-6013	2/7	+ SSc	AL358937
B1.2	Hypothetical gene (LOC91961)	—	+ SSc	XM_041884
B2.1	Translation elongation factor 1 α 1	—	+ SSc	BC021686
B2.2	Chromosome 2, clone RP11-426K3	—	+ SSc	AC016738
B3.1, 3.3	Chorea acanthocytosis, chorein	2/3	+ inv	AF337532
B3.2	Chromosome 15, clone RP11-500C12	—	+ inv	AC090984
B8.1	Lysyl oxidase	—	+ inv	AF270645
B8.2, 8.3	Diacylglycerol kinase	2/3	+ inv	X62535
C1.2	NIRF mRNA for Np95-like rfp	—	+ SSc	AB071698
C1.3	—	—	+ SSc	
C2.1	Chromosome 20, clone RP11-394O2	—	+ inv	AL133227
C2.2	Phospholipase C gamma 1	—	+ inv	NM_002660
C2.3	Chromosome 9, clone RP11-158H18	—	+ inv	AL499602
C3	Class III alcohol dehydrogenase	—/5 (F1)	+ dSSc	M30471
C4.1	Chromosome 11, clone RP11-700F16	—	+ dSSc	AP001775
C4.2	—	—	+ dSSc	
C4.3	Chromosome 22, PAC clone p52f6	—	+ dSSc	AC005500
C5.1	MLN 51	—	+ dSSc	X80199
C5.2	c-cbl protooncogene	2/3	+ dSSc	NM_005188
C6	Fibronectin	3/3	+ dSSc	X02761
D1, E6	Gremlin	3/3, 3/3	+ dSSc	AF110137
D2	Ribosomal Protein, large, RLPO	3/3	— dSSc	NM_001002
D3	Collagen XII alpha 1	3/3	+ SSc	NM_430070
D4	Chromosome 11, clone RP11-775D16	3/3	— dSSc	AP000848
D5	40S ribosomal protein S27 isoform	3/3	— dSSc	NM_015920
E1	Novel gene, chromosome 22	3/3	+ Np	AL050254
E2.1	Chromosome 14, BAC R-307P22	—	+ SSc	AL132777
E2.2, 2.3	Chromosome 14, BAC R-280K24	2/3	+ SSc	AL079307
E3	Zinc finger protein 147 (efp)	3/3	+ dSSc	NM_005082
E5	Cell division cycle 42 (GTP-binding protein, 25kDa)	3/3	+ dSSc	BC018266
E7	Hypothetical gene (LOC116351)	3/3	+ SSc	XM_058000
E8.1, 8.2	KIAA 0477	2/3	+ SSc	AB007946
E8.3	Chromosome 5, clone CTC-325N22	—	+ SSc	AC011351
F1.1	Chromosome 3, BAC RPC11-211P13	— = C3	+ dSSc	AC008249
F1.2	Chromosome 1, clone RP4-675C20	—	+ dSSc	AL157902
F1.3	—	—	+ dSSc	
F1.4	Chromosome 6, clone RP11-235G24	—	+ dSSc	AL391361
F2.1	MEGF5	— = E4	+ inv	AB011538
F2.2	Polymerase II polypeptide B	—	+ inv	XM_028884
F2.3	HSPC 039	—	+ inv	XM_008707

+: increased expression, —: reduced expression, SSc: all patients with SSc, dSSc: only diffuse disease, inv: only involved skin of patients with SSc. Proteins for which a correlation to extracellular matrix production is known are marked in bold.

lysyl oxidase is expressed in involved skin of patients with SSc and less in uninvolved skin or normal skin of healthy persons, confirming both reports and revealing the difference in the level of expression between normal skin and SSc. Of interest, recent data show another aspect of the function of lysyl

oxidase. Giampuzzi, *et al* showed that lysyl oxidase activates the promoter of collagen type III and therefore increases the production of its own substrate¹⁸, suggesting that in SSc increased activity of lysyl oxidase actively supports collagen synthesis. Further, lysyl oxidase is a chemoattractant for

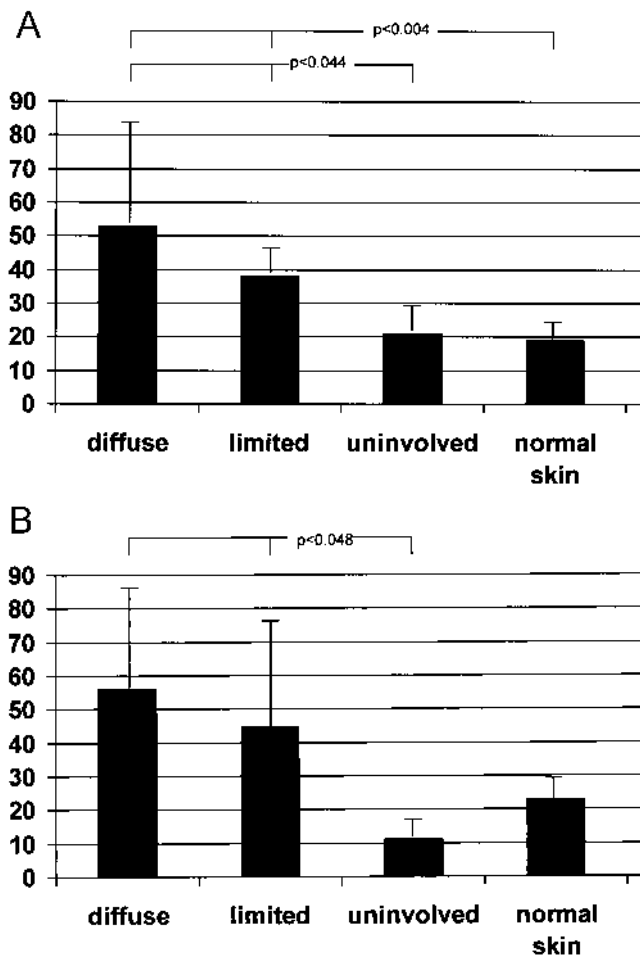


Figure 3. A. Confirmation of differential expression of lysyl oxidase mRNA in SSc and normal skin fibroblast populations by real-time PCR. Values are given by x-fold increase as compared to housekeeping genes. B. Confirmation of differential expression of gremlin mRNA in SSc and normal skin fibroblast populations by real-time PCR. Values are given by x-fold increase as compared to housekeeping genes.

monocytes¹⁹, smooth muscle cells, and fibroblasts²⁰, which may contribute significantly to inflammation by cell migration and increased fibroblast activity.

Gremlin protein. Another interesting protein found to be upregulated in involved skin of SSc is the gremlin protein, whose functions are still unknown to a large extent. A known property of the gremlin protein is antagonizing bone morphogenetic proteins (BMP)²¹, which are members of the transforming growth factor- β (TGF- β) superfamily. There is no known effect on other members of the TGF- β family²². Gremlin binds directly to BMP-2, -4, and -7 and forms heterodimers, thus preventing the receptor binding of the BMP, resulting in inhibition of their activity²¹. Known stimuli for gremlin expression are BMP-2 and BMP-4 as well as the growth factors platelet derived growth factor (PDGF), fibroblast growth factor-2, and TGF- β ²³.

The role of gremlin protein — in concert with BMP — has

been primarily investigated in the regulation of extracellular matrix production in embryogenesis^{24,25}. More recent studies analyzed the role of the cooperation of BMP and gremlin in development of fibrosis in diabetic nephropathy²⁶. Gremlin has been found to be overexpressed in the induction of diabetic nephropathy²⁷ and BMP-7 has been shown to be down-regulated²³. Further, it could be shown in mesangial cells that a decreased activity of BMP-7 results in an increased production of collagen type III and fibronectin²³. Therefore, gremlin appears to exert profibrotic effects in this setting. In addition, the authors could show that the profibrotic growth factor TGF- β induces gremlin and reduces BMP-7²³, subsequently further supporting this imbalance. As gremlin or BMP have not yet been associated with the pathophysiology of SSc, our results show that gremlin is upregulated in involved skin of SSc, and therefore support the hypothesis that gremlin protein may be linked directly to collagen synthesis in SSc.

c-Cbl, *phospholipase C γ 1*, and *DAGK*. Although not significantly dysregulated in the examined samples, these 3 factors might also have the potential to play a role in SSc matrix metabolism. The *c-Cbl* proto-oncogene is an inhibitor of signaling pathways triggered via PDGF and epidermal growth factor^{28,29}. On the other hand, phospholipase *C γ 1* and *DAGK* are important enzymes in cellular signal transduction pathways following stimulation by PDGF³⁰, which is known to induce increased production of collagen in SSc fibroblasts.

In summary, our results show that in addition to the experimental approaches using RAP-PCR for evaluation of differential gene expression in malignant diseases, RAP-PCR for differential display is a suitable and reliable method to identify differentially expressed genes that may have pathophysiological roles in matrix disorders such as SSc.

Moreover, we could identify genes that have not yet been described in the pathophysiology of SSc and are most likely involved in enhanced matrix synthesis and cellular interaction in SSc dermal fibroblasts. Of these, lysyl oxidase and gremlin appear to be the most important.

ACKNOWLEDGMENT

We are indebted to the expert technical assistance of Wibke Ballhorn and Birgit Riepl.

REFERENCES

1. Perucho M, Welsh J, Peinado MA, Ionov Y, McClelland M. Fingerprinting of DNA and RNA by arbitrarily primed polymerase chain reaction: applications in cancer research. *Methods Enzymol* 1995;254:275-90.
2. Kullmann F, Judex M, Ballhorn W, et al. Kinesin-like protein CENP-E is upregulated in rheumatoid synovial fibroblasts. *Arthritis Res* 1999;1:71-80.
3. Preliminary criteria for the classification of systemic sclerosis (scleroderma). Subcommittee for Scleroderma Criteria of the American Rheumatism Association Diagnostic and Therapeutic Criteria Committee. *Arthritis Rheum* 1980;23:581-90.
4. Higuchi R, Fockler C, Dollinger G, Watson R. Kinetic PCR analysis: real-time monitoring of DNA amplification reactions. *Biotechnology* 1993;11:1026-30.

5. Morrison TB, Weis JJ, Wittwer CT. Quantification of low-copy transcripts by continuous SYBR Green I monitoring during amplification. *Biotechniques* 1998;24:954-8.
6. Muller-Ladner U, Judex M, Justen HP, et al. Analysis of gene expression patterns in rheumatoid synovial fibroblasts using RAP-PCR for differential display. *Med Klin (Munich)* 1999;94:228-32.
7. Fleischmajer R, Perlish JS, Krieg T, Timpl R. Variability in collagen and fibronectin synthesis by scleroderma fibroblasts in primary culture. *J Invest Dermatol* 1981;76:400-3.
8. LeRoy EC. Increased collagen synthesis by scleroderma skin fibroblasts in vitro: a possible defect in the regulation or activation of the scleroderma fibroblast. *J Clin Invest* 1974;54:880-9.
9. Kagan HM. Intra- and extracellular enzymes of collagen biosynthesis as biological and chemical targets in the control of fibrosis. *Acta Trop* 2000;77:147-52.
10. Kuivaniemi H, Peltonen L, Kivirikko KI. Type IX Ehlers-Danlos syndrome and Menkes syndrome: the decrease in lysyl oxidase activity is associated with a corresponding deficiency in the enzyme protein. *Am J Hum Genet* 1985;37:798-808.
11. Kagan HM. Lysyl oxidase: mechanism, regulation and relationship to liver fibrosis. *Pathol Res Pract* 1994;190:910-9.
12. Murawaki Y, Kusakabe Y, Hirayama C. Serum lysyl oxidase activity in chronic liver disease in comparison with serum levels of prolyl hydroxylase and laminin. *Hepatology* 1991;14:1167-73.
13. Streichenberger N, Peyrol S, Philit F, Loire R, Sommer P, Cordier JF. Constrictive bronchiolitis obliterans. Characterisation of fibrogenesis and lysyl oxidase expression patterns. *Virchows Arch* 2001;439:78-84.
14. Di Donato A, Ghiggeri GM, Di Duca M, et al. Lysyl oxidase expression and collagen cross-linking during chronic adriamycin nephropathy. *Nephron* 1997;76:192-200.
15. Decitre M, Gleyzal C, Raccurt M, et al. Lysyl oxidase-like protein localizes to sites of de novo fibrinogenesis in fibrosis and in the early stromal reaction of ductal breast carcinomas. *Lab Invest* 1998;78:143-51.
16. Chanoki M, Ishii M, Kobayashi H, et al. Increased expression of lysyl oxidase in skin with scleroderma. *Br J Dermatol* 1995;133:710-5.
17. Kobayashi H, Ishii M, Chanoki M, et al. Immunohistochemical localization of lysyl oxidase in normal human skin. *Br J Dermatol* 1994;131:325-30.
18. Giampuzzi M, Botti G, Di Duca M, et al. Lysyl oxidase activates the transcription activity of human collagen III promoter. Possible involvement of Ku antigen. *J Biol Chem* 2000;275:36341-9.
19. Lazarus HM, Cruikshank WW, Narasimhan N, Kagan HM, Center DM. Induction of human monocyte motility by lysyl oxidase. *Matrix Biol* 1995;14:727-31.
20. Li W, Liu G, Chou IN, Kagan HM. Hydrogen peroxide-mediated, lysyl oxidase-dependent chemotaxis of vascular smooth muscle cells. *J Cell Biochem* 2000;78:550-7.
21. Hsu DR, Economides AN, Wang X, Eimon PM, Harland RM. The *Xenopus* dorsalizing factor Gremlin identifies a novel family of secreted proteins that antagonize BMP activities. *Mol Cell* 1998;1:673-83.
22. Merino R, Rodriguez-Leon J, Macias D, Ganan Y, Economides AN, Hurler JM. The BMP antagonist Gremlin regulates outgrowth, chondrogenesis and programmed cell death in the developing limb. *Development* 1999;126:5515-22.
23. Wang SN, Lapage J, Hirschberg R. Loss of tubular bone morphogenetic protein-7 in diabetic nephropathy. *J Am Soc Nephrol* 2001;12:2392-9.
24. Pereira RC, Economides AN, Canalis E. Bone morphogenetic proteins induce gremlin, a protein that limits their activity in osteoblasts. *Endocrinology* 2000;141:4558-63.
25. Vogt TF, Duboule D. Antagonists go out on a limb. *Cell* 1999;99:563-6.
26. Lappin DW, Hensey C, McMahon R, Godson C, Brady HR. Gremlins, glomeruli and diabetic nephropathy. *Curr Opin Nephrol Hypertens* 2000;9:469-72.
27. McMahon R, Murphy M, Clarkson M, et al. IHG-2, a mesangial cell gene induced by high glucose, is human gremlin. Regulation by extracellular glucose concentration, cyclic mechanical strain, and transforming growth factor-beta 1. *J Biol Chem* 2000;275:9901-4.
28. Broome MA, Galisteo ML, Schlessinger J, Courtneidge SA. The proto-oncogene c-Cbl is a negative regulator of DNA synthesis initiated by both receptor and cytoplasmic tyrosine kinases. *Oncogene* 1999;18:2908-12.
29. Miyake S, Mullane-Robinson KP, Lill NL, Douillard P, Band H. Cbl-mediated negative regulation of platelet-derived growth factor receptor dependent cell proliferation. A critical role for Cbl tyrosine kinase-binding domain. *J Biol Chem* 1999;274:16619-28.
30. Wang Z, Gluck S, Zhang L, Moran MF. Requirement for phospholipase C-gamma 1 enzymatic activity in growth factor-induced mitogenesis. *Mol Cell Biol* 1998;18:590-7.